Solid State Phenomena Vols. 121-123 (2007) pp 561-564
Online available since 2007/Mar/15 at www.scientific.net

doi:10.4028/www.scientific.net/SSP.121-123.561

A comb driving magnetometer based on tunnel effect

TANG Xue-hua[1], YOU Zheng[1],

YANG Yong-jun[2], HE Hong-tao[2]

1 Department of Precision Instruments and Mechanology, Tsinghua University, Beijing 100084, China

2 Micro/Nano Center, Hebei Semiconductor Research Institute, Shijiazhuang, 050051, China

Abstract

In this paper, a comb-driving tunneling magnetometer based on the tunneling effect is introduced. The designation, manufacture and tests of this magnetometer are discussed, including its structure, FEA analysis, machining processes and test results. The test results indicate that the chip is coincidental with the tunneling effect and the chip is capable of sensing the magnetic signal.

Key Words: Tunnel-effect；Magnetometer；MEMS; Comb-driving

Introduction

In the last 15 years the tunneling sensors based on the MEMS technique have been widely explored, such as accelerometers[1-2], gyroscopes[3], uncooled infrared sensors[4] and magnetometer[5-6].

Two types of tunneling magnetometers are reported in the literature, i.e., the vertical and the torsional types. In the vertical one, the direction the magnetic force sensitive is vertical to the structure plane of the device [6], while in the torsional type, there is a torsion arm which senses the magnetic field and rotates around its pivot points [5].

In this work, we develop a novel tunneling magnetometer.

1 Structure

As shown in Figure1, the metal loop is placed on the levers and the mass bulk. The anterior comb fingers are used to draw the mass. Then the gap between the tip electrode and the testing electrode can be made close to the critical value at which the tunneling current is able to be produced. The elastically supported mass system is composed of three parts: the mass bulk, the silicon tip and the lever. There are 4 levers in Figure 1. These levers locate symmetrically at the two sides of the mass bulk. The cantilever or the clip-lever is acceptable. The elastically supported mass system served as the motion-actuate part of the magnetometer is un-contact with the glass wafer and floating in the air. The loop-electrode is used to produce current passing through the metal loop in the magnetometer, while the posterior comb fingers are employed as feedback component for adjusting the value of the tunneling gap.

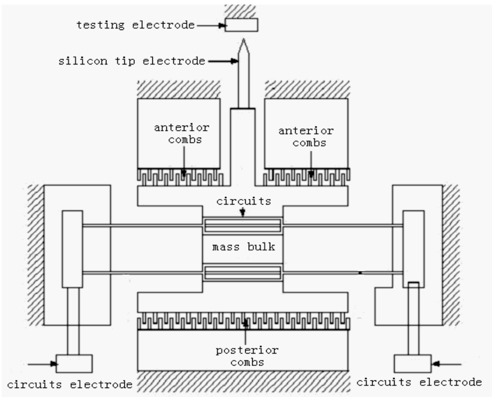

Figure1 main body of the magnetometer

2 FEA Simulations

Basing on the simplification of the elastically supported mass system, we can obtain an analyzed model explained below. In this model we supposed that all the outside forces (referred to the comb-driving force and the Lorenz force in this discussion) applying on the elastically supported mass system are even distributed while the deformation is only referred to the one the levers subjected to, the deformation of the mass bulk in the middle is neglected

Taking the practical processes into account, the static analysis and the model analysis have been carried out in this work. The obtained optimal parameters of the elastically supported mass bulk system are listed as follow: The thickness of the system is 30um, the length of the lever is 750um and its width is 6um respectively. According to the previous supposed model and the counterpart parameters, we provide the results of the vibrate style of the magnetometer using ANSYS FEA tool, as shown in Figure2~5.

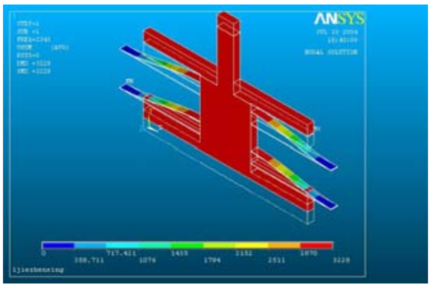

Figure2 1st order vibrate style

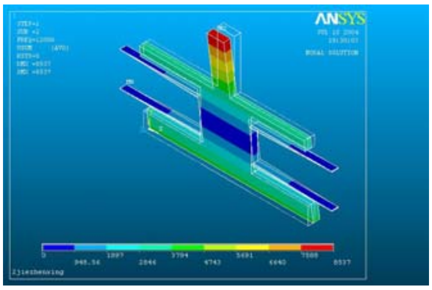

Figure3 2nd order style

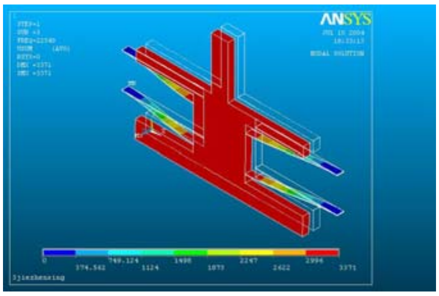

Figure4 3rd order style

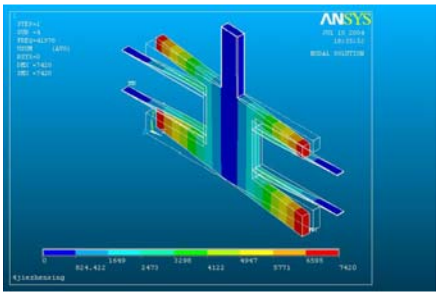

Figure5 4th order vibrate style

As shown in the figures, in 1st order shape, the mass bulk takes on movements parallel to the horizontal direction which defined as the useful movement the magnetometer needed. The mass bulk begins to vibrate from left to right in 2nd order shape. A vertical oscillation appears in the 3rd order shape while the 4th order one is an up-down oscillation.

. All of the movement shapes above except the 1st order one belong to the disturbed motion and should be limited or eliminated to reduce the affect of the structure overlap coupling. Therefore, the working frequency should be restrained less than the 1st resonance frequency.

3 Machining Technology

The novel tunneling magnetometer is fabricated by MEMS bulk process and the detail flow chart is given as follows:

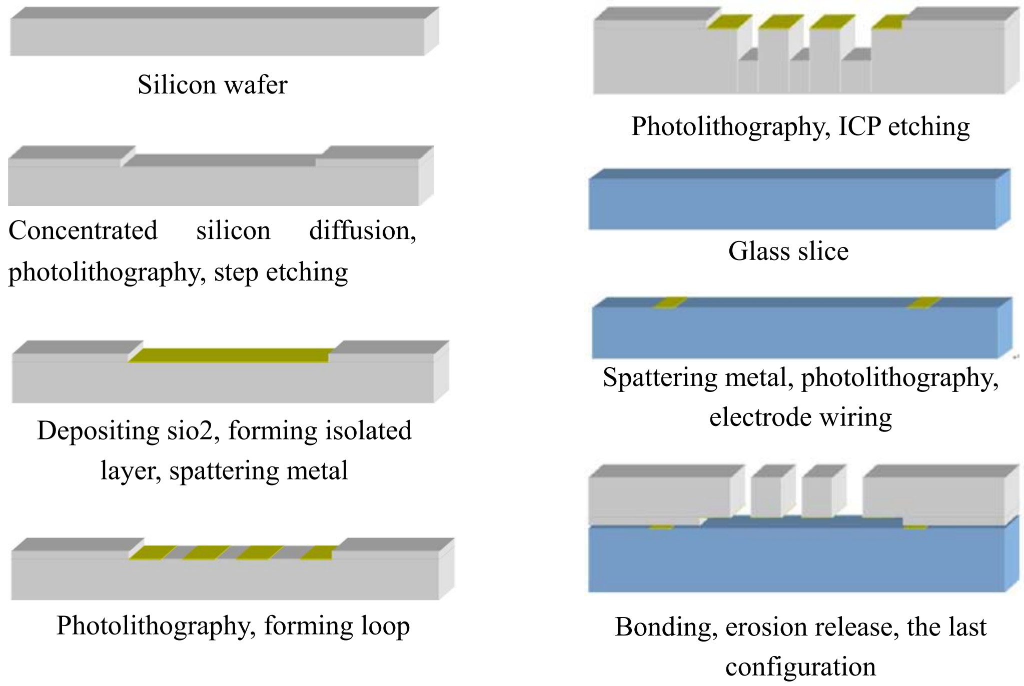

Figure6 Machining Technology

The chips of tunneling magnetometer, based on this technology, had been manufactured and sealed. The size of the sealed chip is 10×6×5mm^3.

Figure7 the sealed chip of the magnetometer

4 Tests and Analysis

(1) The test of relationship between the comb voltage and the tunneling current

When testing, the tunneling electrode was applied a constant voltage of 180mV and the combs were drove by a series of discrete equidistantly increasing voltages called as comb-driving voltage. Figure8 illustrates the testing result of a certain chip and from which it is clear to see that the nA level of the tunneling current appears only if the driving voltage is not less than 63V.

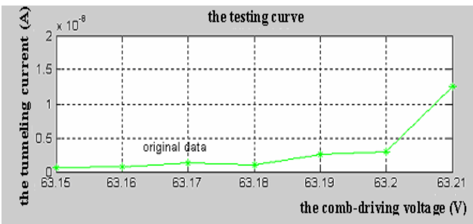

Figure8 testing data about the tunneling current and the comb-driving voltage

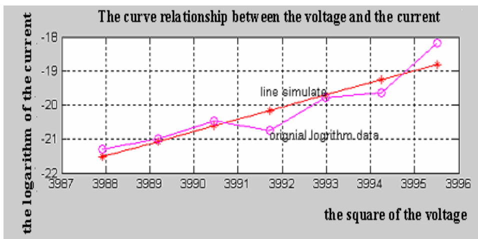

Figure9 relationships between the logarithm of the tunneling current and the square of the comb-driving voltage

Figure9 displays the relationship between the square of the driving voltage and the logarithm of the tunneling current. The result of the fitting linear line to the crude data gives a rate of slope C of 0.3591, an intercept C_0 of 1453.7 and a fitting coefficient of 0.93. Such relative high fitting coefficient implies that the logarithm of the tunneling current and the square of the driving voltage have a linear relation. Basing on the analysts, the tunneling effect appears during the test[2].

（2）the test of relationship between the coil current and the tunneling current

When testing, the tunneling electrode and the combs were applied voltages of 180mV and 59V respectively and these values will keep constant through the tests. Then the observation was setting up while a series of scanning current was activated in the coils. Figure10 bases on the crude data getting from the observation while the amplitude of the coil current is between 10mA and 20mA.

In theory, the tunneling current should be a sum of two parts, one is related to the comb-driving voltage (induced by the comb-driving force) and the other is related to the coil current (induced by the Lorentz force). But in this period of tests the tunneling current was only generates by the coil current because in the previous test about the relationship between the comb-driving voltage and the tunneling current it had been cleared that the tunneling current would be ignored if the comb-driving voltage was lower than 63V which was remarkably higher than the current 59V.

Because the tunneling current in figure 3 was induced by Lorentz force, the tunneling magnetometer chip under testing is able to sense the magnetic signal.

As shown in the figure10, the horizontal axis is about mA level of scanning currents with every grid representing 1mA while the vertical axis is about nA level of tunneling currents with every grid representing 2nA (the tunneling currents were restricted under 20nA in the tests).

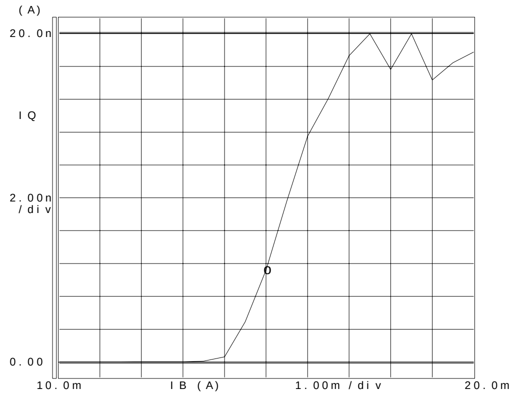

Figure10 testing diagram about the tunneling current and the coil current

Conclusion

This paper provides a new designation of tunneling magnetometer. Following such design, we have finished the designation, the manufacture and the primary testing. The testing results indicate that we have actually obtained some eligible products, whose testing data can satisfy the tunneling effect and can sense the magnetic signal. It is possible that by calibrating the magnetometers in a known weak magnetic field the testing precision of such tunneling magnetometers can be settled.

References

[1] C. H. Liu, T. W. Kenny, A high-precision, wide-bandwidth micro machined tunneling accelerometer, in: Journal of Microeletromechanical Systems, 2001, 10(3): 425-433.

[2] P. G. Hartwell, F. M. Bertsch, S. A. Miller, et al, Single mask lateral tunneling accelerometer, in: Proceedings of the IEEE Micro Electro Mechanical Systems (MEMS), IEEE, 1998:340~344

[3] R. L. Kubena, J. Vickers-kirbyd, R. J. Joyce, et al, New tunneling –based sensor for inertial rotation rate measurements, in: Sensors and Actuators, A: Physical, 2000, 83(1): 109-117.

[4] T. W. Kenny, J. K. Reynolds, J. A. Podosek, et al, Micromachined infrared sensors using tunneling displacement transducers, in: The Review of Scientific Instruments, 1996, 67(1): 112-128.

[5] D. DiLella , L.J. Whitman , R.J. Colton ,et al. A micro-machined magnetic-field sensor based on an electron tunneling displacement transducer, in: Sensors and Actuators, A: Physical, 86(1-2), 2000: 8–20

[6] L. M. Miller, T. W. Kenny, J.A. Kovacich, et al, A μ- Magnetometer Based on Electron Tunneling, in: Proceedings 1996 IEEE- MEMSWorkshop, 467~471.

Nanoscience and Technology
10.4028/www.scientific.net/SSP.121-123

A Comb Driving Magnetometer Based on Tunnel Effect
10.4028/www.scientific.net/SSP.121-123.561

DOI References

[5] D. DiLella , L.J. Whitman , R.J. Colton ,et al. A micro-machined magnetic-field sensor based on an lectron tunneling displacement transducer, in: Sensors and Actuators, A: Physical, 86(1-2), 2000: 8–20
doi:10.1016/S0924-4247(00)00303-4
[4] T. W. Kenny, J. K. Reynolds, J. A. Podosek, et al, Micromachined infrared sensors using tunneling displacement transducers, in: The Review of Scientific Instruments, 1996, 67(1): 112-128.
doi:10.1063/1.1146559